Biological Trace Element Research (2025) 203:467–484
https://doi.org/10.1007/s12011-024-04168-7

RESEARCH

Biosynthesis Optimization of Antibacterial-Magnetic Iron Oxide Nanoparticles from *Bacillus megaterium*

Sajedeh Hajiali[1] · Sara Daneshjou[2] · Somayeh Daneshjoo[3] · Khosro Khajeh[4]

Received: 28 January 2024 / Accepted: 31 March 2024 / Published online: 12 April 2024

Abstract

The occurrence of antibiotic resistance on common bacterial agents and the need to use new generations of antibiotics have led to the use of various strategies for production. Taking inspiration from nature, using bio-imitation patterns, in addition to the low cost of production, is advantageous and highly accurate. In this research, we were able to control the temperature, shake, and synthesis time of the synthesis conditions of *Bacillus megaterium* bacteria as a model for the synthesis of magnetic iron nanoparticles and optimize the ratio of reducing salt to bacterial regenerating agents as well as the concentration of salt to create iron oxide nanoparticles with more favorable properties and produced with more antibacterial properties. Bacterial growth was investigated by changing the incubation times of pre-culture and overnight culture in the range of the logarithmic phase. The synthesis time, salt ratio, and concentration were optimized to achieve the size, charge, colloidal stability, and magnetic and antibacterial properties of nanoparticles. The amount of the effective substance produced by the bacteria was selected by measuring the amount of the active substance synthesized using the free radical reduction (DPPH) method. With the help of DPPH, the duration of the synthesis was determined to be one week. Characterizations such as UV–vis spectroscopy, FTIR, FESEM, X-ray, and scattering optical dynamics were performed and showed that the nanoparticles synthesized with a salt concentration of 80 mM and a bacterial suspension to salt ratio of 2:1 are smaller in size and have a light scattering index, a PDI index close to 0.1, and a greater amount of reducing salt used in the reaction during one week compared to other samples. Moreover, they had more antibacterial properties than the concentration of 100 mM. As a result, better characteristics and more antibacterial properties than common antibiotics were created on *E. coli* and *Bacillus cereus*.

Keywords Biomimetics · *Bacillus megaterium* · IONPs based · Optimization · Antibacterial nanomaterial

Introduction

Nosocomial infections occur during hospitalization or as a result of hospitalization. They come to the hospital after 48 h and are among the most important causes of death, the death rate, and the increase in the number of hospitalization days and the cost of treatment. *B. cereus* causes severe non-gastrointestinal infections such as bacteremia, endocarditis, meningoencephalitis, and pneumonia. Severe infections occur, especially in immunocompromised patients, sometimes leading to nosocomial infections. Such nosocomial infections with *B. cereus* have been reported to be associated with *B. cereus* contamination of ventilator equipment, intravenous catheters, and linen [1]. On the other hand, *B. ceeusis* is able to resist the main disinfectants, grow at top temperature, and the formation of biofilm in industry or biomedicine. Machines are, therefore, often found in food-processing hospital settings. Pollution related to biomedical devices may be the cause of hospital infections [2]. The synthesis of nanoparticles from biological sources such as bacteria, fungi, algae, yeasts, and plants is considered a valuable method because it does not have the possible health and environmental risks of other methods, and

✉ Sara Daneshjou
s.daneshjou@modares.ac.ir

1 Department of Nanotechnology, Faculty of Advanced Sciences and Technology, Tehran Medical Sciences, Islamic Azad University, Tehran, Iran

2 Department of Nanobiotechnology, Faculty of Biological Science, Tarbiat Modares University, Tehran, Iran

3 Department of Medical Nanotechnology, Faculty of Advanced Sciences and Technology, Tehran Medical Sciences, Islamic Azad University, Tehran, Iran

4 Department of Biochemistry, Faculty of Biological Science, Tarbiat Modares University, Tehran, Iran

low-cost production sources are used [3]. The use of bacteria as a source of metal nanoparticle production is of particular importance [4]. Magnetic nanoparticles, which occupy a large part of nanomaterials, have the potential to revolutionize clinical diagnosis and treatment due to their unique properties, such as magnetic resonance, superparamagnetic momentum, and the power of biological interactions at the cellular and molecular levels [5–9]. Because of their unique characteristics, magnetic nanoparticles have attracted much attention, and as the design of the route for the synthesis of nanoparticles creates different characteristics in them, researchers have developed different routes for the synthesis of magnetic nanoparticles for use in biotechnology. Magnetic nanoparticles have been used in the fields of pharmaceuticals, computers, water, and wastewater treatment, among others, so far, and each use has advantages and limitations [7–12]. Among the biosynthesized metal nanoparticles, gold and silver are among the most important ones, and many articles have been devoted to their use in the field of biosynthesis with various applications in improving diagnostic and therapeutic methods [10–18]. Nonetheless, iron oxide nanoparticles are used in pharmaceutical research because of their appropriate magnetic properties, low toxicity, high compatibility, and relative ease of synthesis compared to other metals [19–24]. Moreover, because of its magnetic properties, iron oxide has diagnostic capabilities, can simultaneously perform targeted drug delivery in addition to disease diagnosis, immunoassay, drug delivery, and detoxification of biologic fluids, and can be easily recovered from the reaction mixture by applying an external magnetic field [5, 9, 25]. Targeted medicine reduces toxic side effects in non-diseased areas and keeps the systemic effect at the lowest level, usually to prevent the accumulation of iron nanoparticles and create superior features in targeted drug systems and surface gene therapy. These nanoparticles are covered with different coatings [26, 8, 27, 28]. So far, various chemical synthesis methods have been used to produce pure iron nanoparticles, iron alloys, and iron oxides in addition to green synthesis methods for producing iron oxide nanoparticles (IONPs), such as the use of ginger root (*Zingiber officinale*), neem leaf (*Azadirachta indica*), or the biosynthesis of iron oxide by the cytoplasmic extract of *Lactobacillus fermentum*, which is a probiotic microorganism [28–33]. So far, many researches have been conducted on the production of nanoparticles from different sources; a group of these researches use biological sources for the synthesis of nanoparticles. Among biological resources, the use of bacteria to make nanoparticles is common, but the ethical principles in using biological resources, on the one hand, the volume of synthesis, on the other hand, in addition to the production of nanoparticles with the size, uniformity, and stability of these nanoparticles are always research challenges. Among the researches carried out on the synthesis of nanoparticles from gram-positive bacteria and the *Bacillus* branch, it is possible to focus on *Bacillus megaterium* as a source of nanoparticle production for the reasons stated below. Iron-oxidizing bacteria are found among both gram-positive and gram-negative groups. Iron-oxidizing bacteria convert ferrous ions to ferric, and different species do this at different rates. Microbial oxidation of iron can be done in both aerobic and anaerobic environments [34]. *Bacillus megaterium* is deeply rooted in the *Bacillus phylogeny*, making it an evolutionary important *Bacillus* species. This organism was introduced as a gram-positive model organism long before *Bacillus subtilis*. Unlike gram-negative organisms such as *Escherichia coli* (*Escherichia coli*), *Bacillus megaterium* does not produce endotoxin during outer membrane growth, so it is used as a non-pathogenic commercial host for the production of biotechnological products and also biochemical studies [35]. *Bacillus* are one of the important sources of production of natural products with antimicrobial activity that are found in various habitats, and they can even be seen among the diversity of marine microorganisms. Bacilli belong to the *Bacillus* family, which are rod-shaped, gram-positive, catalase-positive, and facultatively anaerobic. *Bacillus* bacteria can spread in various habitats by producing endospores. They can also survive harsh environmental conditions such as strong sunlight, dryness, and extreme heat [36]. Phycosynthesis or synthesis of iron nanoparticles by algae is a sustainable, environmentally friendly, and non-toxic approach. After exposure to a precursor solution, the biomolecules in these organisms act as reducing and capping agents, leading to the production of nano-iron. For microscopic unicellular algae, intracellular synthesis by means of live cell suspensions is often favored, and macroalgae such as seaweed are utilized as cell-free extracts to stimulate extracellular production. More than ten Phyophis species have been found to produce iron nanoparticles in cell-free extract conditions. As reported so far, different genera from different branches of algae are able to produce iron nanoparticles [37]. But the *Bacillus* genus, the main representative of endospore-forming aerobic bacteria, is one of the most diverse genera that currently consists of 273 valid species. Bacilli, originally described as soil bacteria, can be enriched in almost any environment and contain numerous species that are useful in agriculture, food industry, and food processing [38]. The current research was an attempt to obtain a more effective substance from *Bacillus megaterium* by optimizing the conditions of bacterial culture for the regeneration of iron II sulfate salt as the salt used in synthesis. We were able to optimize the conditions of synthesis of iron oxide nanoparticles with the help of the crystallization pattern in the bacterium *Bacillus megaterium* and by using iron sulfate II salt; nanoparticles with a more stable index are more favorable by examining the salt

concentrations and volume ratios common in various areas of research. Furthermore, they are produced in a smaller size. The first step in this research was to optimize bacterial growth conditions by synthesizing iron oxide magnetic nanoparticles. In the second step, the amount of reducing agent in the extracellular extract of the bacteria was measured, and it was added to the iron sulfate II salt solution in different ratios. Finally, the best ratio was selected for the cell extract mixture with Ec50. In the third step, we examined the effect of the iron II sulfate salt concentration in the synthesis and added a salt solution in four concentrations with the ratio obtained in the previous step. In this way, we obtained the optimal concentration in the ratio of 2:1. In the fourth step, we investigated the antibacterial properties of the synthesized nanoparticles. The produced nanoparticles have effective antibacterial properties against gram-positive and gram-negative strains by disking, well, and MIC methods in comparison with both the controls and the standards mentioned in the tables. Nadagouda et al. recognized and evaluated to investigate the additive properties of the instant antibiotic disc impregnated with nanoparticles [39].

Material and Methods

Optimizing the Growth Conditions of Bacteria to Achieve a Higher Amount of Regenerator

Synthesis of *Bacillus megaterium* bacterium (*Bacillus megaterium* PTCC1250) from the standard bacterial strain was produced in the collection center of fungi and industrial and infectious bacteria of Iran Scientific and Industrial Organization in the microbial culture medium Nutrient Broth (LB broth) produced by Merck Germany based on the standard ratio and incubated as described in Table 1 (i.e., time period of 10 to 24 h and temperature range of 30 to 40 degrees (30 ℃, 33 ℃, 37 ℃, 40 ℃) with movement between 120 and 200 rpm separately for each of the factors of time, temperature, and stirring in all mentioned conditions). Then, the cultured bacteria under different conditions were centrifuged at 5000 rpm for 20 min to obtain the extracellular suspension of the bacteria. The supernatant liquid was collected in sterile containers and dried at 80 °C in an OF-01E model dry oven from JEIO TECH Company, Korea, and the DPPH (1, 1-diphenyl-2-picrylhydrazyl) test by DPPH Merck Germany was used to measure the reducing power. To perform this test, the samples were centrifuged at specific time intervals, and the supernatant was used to perform the DPPH test. Salt reduction is performed by reducing agents, and the synthesis will continue as long as the reducing agents have the ability to accomplish the reaction. The effective substance means salt-reducing agents that exist in the extracellular suspension of *Bacillus* bacteria. After centrifugation, the extracted bacterial suspension is collected in a sterile container, and after the passage of time, it is removed from them at appropriate time intervals, poured into the well of a 96-well plate, and placed in a dark room. They were treated with DPPH, and after 30 min, they were read by an ELISA reader at 560 nm wavelength. Spectrophotometric measurement of the change in DPPH absorption on the sample, the initial culture medium sample, the culture medium without bacterial residues after bacterial growth, and the sample resulting from the separation of bacterial biomass, 50% ethanol DPPH solution as a control, and the remaining solution after being separated from the bacterial suspension were performed in each of the cultured samples in different conditions immediately after centrifugation and also after every seven hours up to one week. The blank of each sample was equal to 96% ethanol, the desired sample was considered for absorption reading, and finally, the best sample that had the highest amount of oxidizing agents within a week was selected, and the bacterial growth conditions based on that sample as optimal growth condition bacteria were selected. In order to calculate the regenerative power of each sample, the 35% DPPH inhibition index was used. After comparing the results obtained from the analysis of the amount of regenerating power, the time, temperature, and degree of movement suitable for bacterial growth were determined to achieve the maximum amount of regenerating agent in the suspension resulting from bacterial growth.

Table 1 Synthesis of *Bacillus megaterium* bacterium (*Bacillus megaterium* PTCC1250) in the time period of 10 to 24 h and temperature range of 30 to 40 degrees with movement between 120 and 200 rpm separately for each of the factors of time, temperature, and stirring in all mentioned conditions

Factor									
Time	Hour	10	12	14	16	18	20	22	24
	Code	H1	H2	H3	H4	H5	H6	H7	H8
Temperature	Centigrade	30°		33°		37°		40°	
	Code	T1		T2		T3		T4	
Shake	Round per minute	120 $r.min^{-1}$		150 $r.min^{-1}$		180 $r.min^{-1}$		200 $r.min^{-1}$	
	Code	S1		S2		S3		S4	

Nanoparticle Synthesis from Extracellular Extract and Salt Solution

After the growth of the bacteria according to the results of the previous step, the suspension of the bacteria with the solution of iron (II) sulfate (iron (II) sulfate) from Merck, Germany, with a final concentration of 0.1 M was mixed at ambient temperature, neutral pH, and with different ratios of 1:1, 1:2, 1:3, 1:4 (for the synthesis of iron oxide nanoparticles and investigation of the effect of volume ratio of suspension to salt in the synthesis) and removed from the solution at different time intervals. It was then centrifuged from the supernatant to the amount suitable for measuring. The total regenerator remaining in the solution was removed and compared with the control sample (suspension without adding salt). The duration of synthesis and the strength of regenerator activity were investigated using visible-ultraviolet light spectroscopy (UV–vis spectroscopy) in the range of 200 to 700 nm by Perkin-Elmer spectrophotometer. All samples were first separated from the soup by centrifugation to perform image and spectroscopic characterization methods and then washed with distilled water and centrifuged again. after the washing process, it was repeated three times. After centrifuging three times, the produced samples were collected in sterile containers and dried at a temperature of 25 ℃ in an OF-01E drying oven from JEIO TECH, Korea. In this research, all tests were repeated 3 times, and the results were expressed as the average of three repetitions ± standard deviation. The analysis of variance (ANOVA) test was used for statistical analysis of the results. The precipitate obtained from centrifuging was analyzed by Fourier transform infrared spectroscopy (FTIR; Thermo Scientific, USA; Model: Nicolet IR100) to ensure the synthesis of iron oxide nanoparticles. The results showed that iron nanoparticles were produced at ambient temperature immediately after salt was added to the suspension. Furthermore, at ratios of 1:1 and 1:2, a lower amount of residual regenerator was observed in the supernatant solution. To select the appropriate ratio of bacterial suspension and saline solution, the samples were imaged with an FESEM field emission scanning microscope under equal conditions. The previous steps were repeated from the beginning after ensuring the condition of the resulting samples, and after filtration, any biological residue was removed by transferring the appropriate amount of suspension-containing nanoparticles onto the slide with the help of a capillary tube and after drying. Images were taken with the FESEM of ZEISS, Germany, Sigma VP model, and the size of the samples was determined in two scales of 100 nm and 200 nm.

Optimization of Salt Concentration in Synthesis

Nadagoda et al. investigated the effect of tea extract and salt concentrations on the size of iron nanoparticles and reported that by changing the concentration of the extract and salt, the size and shape of nanoparticles change [40]. The appropriate volume ratio of salt and suspension was determined for a concentration of 0.1 M (100 m mol). We also investigated the concentrations of less than 0.1 M (50 mM and 80 mM) and 1 M (1000 mM) based on the research of Saravanan et al. in the synthesis of zinc nanoparticles with *Bacillus megaterium* bacteria and the same ratio of 2:1 suspension bacteria to salt [41]. We further investigated the effect of changing the concentration of extract and salt on the size and shape of synthesized iron oxide nanoparticles. UV–vis spectroscopy (using a Perkin-Elmer spectrophotometer, Perkin Elmer, USA, Model: lambda 25) in the range of 200 to 700 nm was used to compare the synthesized iron oxide nanoparticles. Fourier transform infrared spectroscopy or FTIR imaging with field emission scanning microscope FESEM by FESEM device (ZEISS, Germany), model Sigma VP, was used for imaging and size determination in two scales of 100 nm and 200 nm. With the help of X-ray energy-dispersive spectroscopy (EDS), simultaneously with observing the image and morphology of the sample, a two-dimensional elemental map of the sample was created by transmission electron microscope as a side technique, and qualitatively and quantitatively, the spatial distribution of the elements on the surface of the samples and optical dynamic scattering (DLS) were examined. The size of the particles was determined by measuring the Brownian motion of the particles or the displacement of the nanoparticles in the suspension by Zeta-DLS (Zetasizer model, Malvern, UK). The zeta potential of nanoparticles was analyzed as an index to determine the stability of the sample and the size of the nanoparticles [42–44]. Finally, after examining the results of all the analyses performed, the appropriate concentration was selected to obtain the most desirable nanoparticle with confidence, and X-ray diffraction (XRD) and crystal structure characterization of the nanoparticles was done with the X Pert Pro XRD device of the Panalytical Company.

Examining the Antibacterial Properties of the Synthesized Nanoparticles

After centrifuging three times, the produced samples were collected in sterile containers and dried at a temperature of 25 ℃ in an OF-01E drying oven from JEIO TECH, Korea. Then, antimicrobial susceptibility test discs containing antibiotics manufactured by Padtan Teb Co. and produced in Tehran, Iran, were used, and BLANK PAPER DISCs impregnated by Merk Germany with iron oxide nanoparticles and control samples 6.4 mm in size, similar to the size of the antibiotic discs, were prepared in a sterile environment. Antibacterial tests by the disc diffusion method were performed on Mueller Hinton agar medium plates by Merk Germany to investigate the antibacterial activity of synthesized iron oxide nanoparticles, a biomimetic method

for clinical applications and disinfection in comparison with industrial antibiotics, on two strains of gram-positive and gram-negative bacteria, *Bacillus cereus* (ATCC14579), and *E. coli* (ATCC 25922) bacteria. For this purpose, first, the isolated bacteria were cultured in a blood agar medium for 24 h. After ensuring the turbidity of half of the McFarland sample, it was cultured by sterile swab next to the flame and under the microbiology hood on Mueller Hinton agar medium in all directions. The plates were placed at room temperature for 5–10 min to absorb the moisture. Then, the used antibiotic discs, which had been frozen in advance at − 20 °C, were removed and allowed to reach ambient temperature. Using sterile tweezers, they were placed next to the flame and under the microbiology hood on the surface of the plate at a distance of 20 mm from the plate edge and 25 mm from each other. The discs were then incubated at 35 °C, and the results were analyzed after 18 h. After obtaining assurance of the antibacterial property of the synthesized sample, in order to determine the inhibitory power of nanoparticles, the micro-broth dilution method was used to determine the minimum lethal concentration or MIC (minimal inhibition concentration), and the well diffusion method was also performed on the bacteria. For the micro-broth dilution method, a sterile 96-well plate was used to determine MIC. Consecutive dilutions of the nanoparticle solution with a volume equal to the volume of the microbial suspension and Mueller Hinton broth were poured into each well and incubated for 20 h at 37 °C. Mueller Hinton Agar medium by Merk Germany with each type of bacteria in an independent well served as a negative control for each bacteria, and the antibiotic effective on that bacteria used in the antibacterial test by disking method was used along with bacterial suspension in another well to compare the retention power of the antibiotic with nanoparticles. Finally, after the incubation time, the 96-well plate was read by the FCC Compliance device from BioTek at a wavelength of 500 nm. In the well diffusion method, the Mueller Hinton Agar culture medium of Merck Company was used, and using sterile swabs, bacteria were cultured with a concentration of half McFarland on the plates in all directions. Then, using a sterilized pipette number 5, wells with a diameter of 4 mm were created on the culture medium; 30 µL (0.03 ml) of the desired nanoparticle sample was placed inside them with concentrations equivalent to those that inhibited the growth of the desired bacteria in the MIC method. Moreover, the control Ha was inoculated. The samples were then incubated for 24 h at 37 ℃. Finally, the diameter of the inhibition halos of nanoparticles and controls was measured with calipers, and which concentration in the MIC method has the power to create a halo of non-growth by a few millimeters was determined.

Results

In this study, all tests were repeated 3 times, and the results were expressed as the average of three repetitions ± standard deviation. The analysis of variance (ANOVA) test was used for statistical analysis of the results. The results were analyzed by SPSS 20 software, and $P < 0.05$ was considered significant.

Optimizing the Growth Conditions of Bacteria to Achieve a Higher Amount of Regenerator

The antioxidant power of the available extracts was determined by changing the purple color of the aqueous solution of diphenyl picrylhydrazyl to yellow. The solution was stirred at a low speed and room temperature without light, and after 30 min, 60 min, and 90 min, the absorbance of the solutions was measured at a wavelength of 517 nm, and the inhibition percentage was calculated based on the following formula:

$$IP\% = ((A\,\text{blank} - A\,\text{sample})/A\,\text{blank})(100)$$

IP% : antioxidant inhibition percentage against free radicals

A blank(control absorption) : 2 ml of distilled water in 2 ml of DPPH solution

A sample : (sample absorption)

Measuring the reductive power obtained from the DPPH test of the samples indicated the maximum amount of the effective bio-inspiring agent for nanoparticle synthesis in a 12-h overnight synthesis at 37 °C with a shaking power of 180 rpm (H2T3S3 sample) as the optimal conditions for bacterial growth, which were considered in the following research.

Synthesis of Iron Oxide Nanoparticles by *Bacillus megaterium* Bio-regenerators

The reaction of the 0.1 M iron sulfate salt and bacterial suspension with volume ratios of 1:1, 2:1, 3:1, and 4:1, at ambient temperature, in the range of 25 ℃, and neutral pH, for the synthesis of iron oxide nanoparticles and investigating the effect of the ratio volumetric suspension to salt was performed in the synthesis. At the very beginning of the reaction, the

Fig. 1 0.1 M iron II sulfate salt in light yellow color

color of the salt solution (Fig. 1) changed from light yellow (Fig. 2) to dark brown (Fig. 3). This color change is the first sign of the formation of iron oxide nanoparticles [45]. After that, volume ratios of 1:1, 2:1, 3:1, and 4:1 were prepared for the mixture consisting of fixed salt volume ratio and different suspension ratios at ambient temperature, according to Table 2. After 20 min, 1 h, 12 h, one day, and up to two weeks, the reaction rate of salt and regenerator in the suspension was checked in two manners. In the first method, the sample was centrifuged, and the amount of regenerator remaining in the supernatant liquid, which failed to reduce the salt, was measured from the supernatant solution and compared with the amount of regenerator in the control sample. The results of this route are shown in Fig. 2, from the moment of the addition of salt to the bacterial suspension solution when the amount of regenerator in the supernatant was at its maximum. With the passage of time and the measurement of the amount of regenerator in the samples being synthesized, a gradual

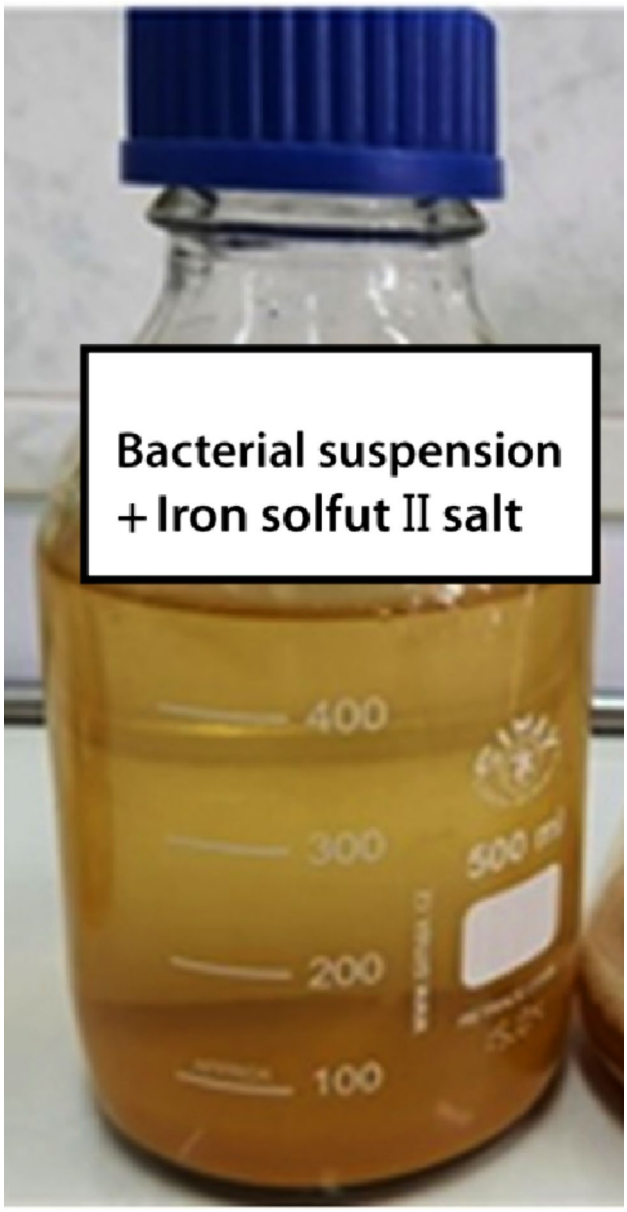

Fig. 2 Bacterial suspension in clear yellow color

decrease in the amount of regenerator in all volume ratios was observed. It was also observed that in the volume ratio of 2:1 bacterial suspension (2) to salt (1) after one week, the amount of regenerator in the supernatant remained constant, and in all ratios after two weeks, the number read by the device was zero. The control sample, however, the suspension of which contained no salt, still had the reducing power of about 60% iodine after two weeks, which can be attributed to the low quality of the reducing agent in the presence of nanoparticles. The particles were considered the inhibitory agent for the activity of reductive agents and reaction with DPPH.

In the second method, we separated the sediment resulting from centrifuging the samples at the same time, and

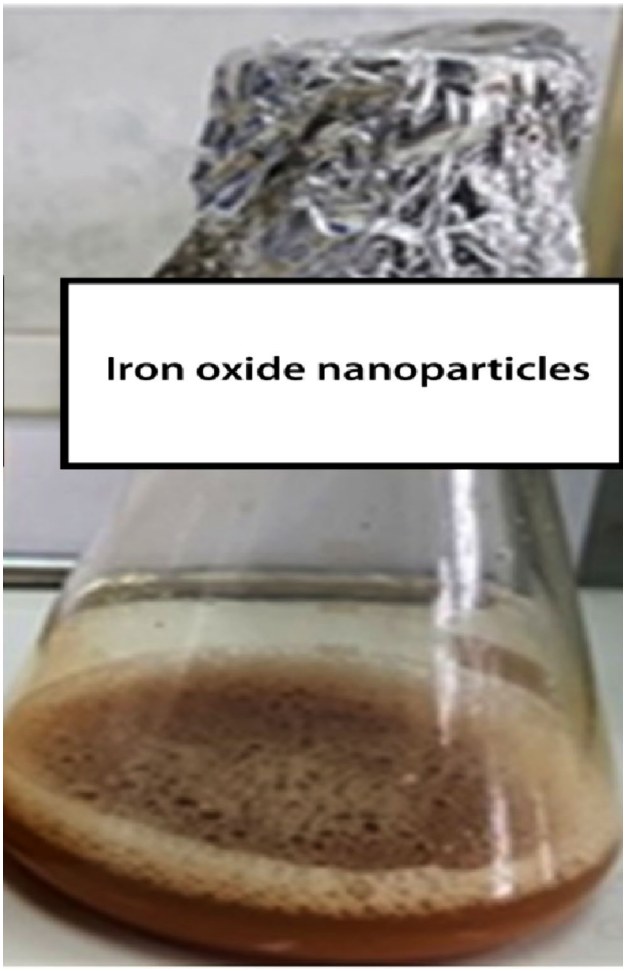

Fig. 3 Reaction mixture of bacterial suspension and salt containing iron oxide nanoparticles in dark brown color

after washing three times with distilled water and repeating the centrifugation process, it was passed through filter paper and a 0.22-micron filter. Then, using visible-ultraviolet light spectroscopy (UV–vis spectroscopy), the sediment was characterized in the range of 200 to 700 nm. The results of this investigation are shown in Fig. 4. The comparison revealed two main points. First, with the passage of time in all the volume concentration samples, an increase in the height of the peak was observed, which indicated that the progress of the reaction between the bacterial regenerator of salt and the salt in the sample container was our synthesis. Second, the increase of the peak remained constant after a period of time. By comparing these points with the points where the amount of regenerator remaining in the supernatant remains constant (first path), we found in all samples that after one week, the height of the peak did not change further, which can reduce the amount of regeneration power, and this is related to the regeneration of salt. As the one-week period got closer, the curve became wider, which can be explained by the agglomeration of nanoparticles [46]. Finally, it was determined that the appropriate volume ratio is 1:2 of suspension (2) to salt (1). As shown in Fig. 4, at the same time, there is not much difference in terms of the size of nanoparticles with a ratio of 1:1, but the height of the peak observed according to Fig. 4 is higher compared to the ratio of 1:1. In addition, the widening that is observed in other volume ratios was not observed in the 2:1 ratio. Moreover, the two ratios of 1:2 and 1:4 had the highest peak height, so FESEM imaging was done to check the size of nanoparticles from these two samples. As can be seen in Fig. 5, the nanoparticles were larger in size in the 1:4 ratio but smaller in size in the 1:2 ratio.

Optimization of Salt Concentration in Synthesis

After determining the appropriate volume ratio of salt and suspension (2:1), in the synthesis of nanoparticles with a final concentration of 0.1 M (100 mM) iron sulfate salt, concentrations of 50 mM, 80 mM, and 1000 mM (1 M) of salt were mixed with bacterial suspension at a volume ratio of 2:1 with neutral pH and at ambient temperature. In all samples, a color change was observed immediately after salt was added to the bacterial suspension. UV–vis spectroscopy in the range of 200 to 700 nm indicated the presence of iron nanoparticles in the range of 320 to 420 (Fig. 6) and was examined at intervals of up to one week. As shown in Fig. 6, in samples with higher salt concentration, the spectrum was shifted to longer wavelengths or red shift, which indicated the larger size of the particles in

Table 2 Numerical values and codes related to the volume ratio of bacterial suspension and the final salt concentration of 0.1 M in ratios of 1:1, 1:2, 1:3, and 1:4

Fixed salt: variable suspension ratio	Salt concentration in each ratio	The volume of the reaction mixture	Weight of salt present in each ratio	Volume of salt solution	Volume of bacterial suspension	Sample code no
1:1	0/1 M	10 ml	3/336 g	5 ml of 1.2 M salt	5 ml	A
1:2	0/1 M	10 ml	0/832391 g	3/34 ml of 0.2994 M salt	6/66 ml	B
1:3	0/1 M	10 ml	1/11208 g	2/5 ml of 0.4 M salt	7/5 ml	C
1:4	0/1 M	10 ml	1/3901 g	2 ml of 0/5 M salt	8 ml	D

The amount of salt is the same volume of saline solution to maintain the final concentration of salt in all proportions

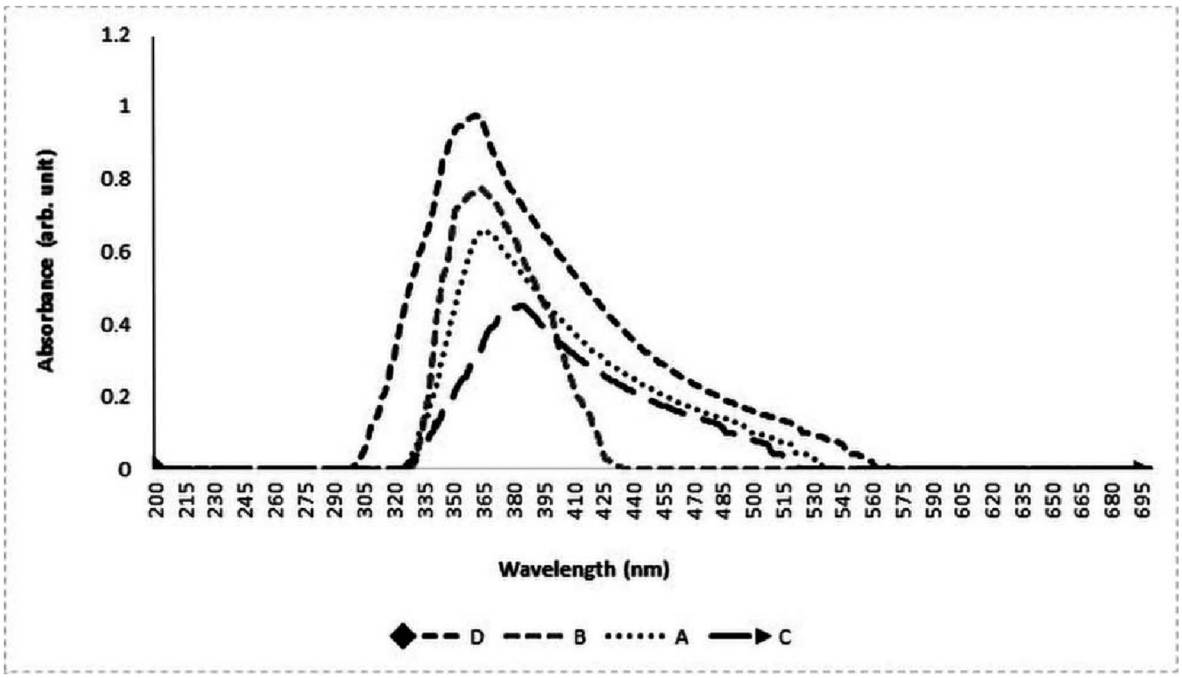

Fig. 4 Ultraviolet–visible spectroscopy (UV–VIS) of four samples of fixed salt volume ratio and variable bacterial suspensions, codes A, B, C, and D, according to Table 2

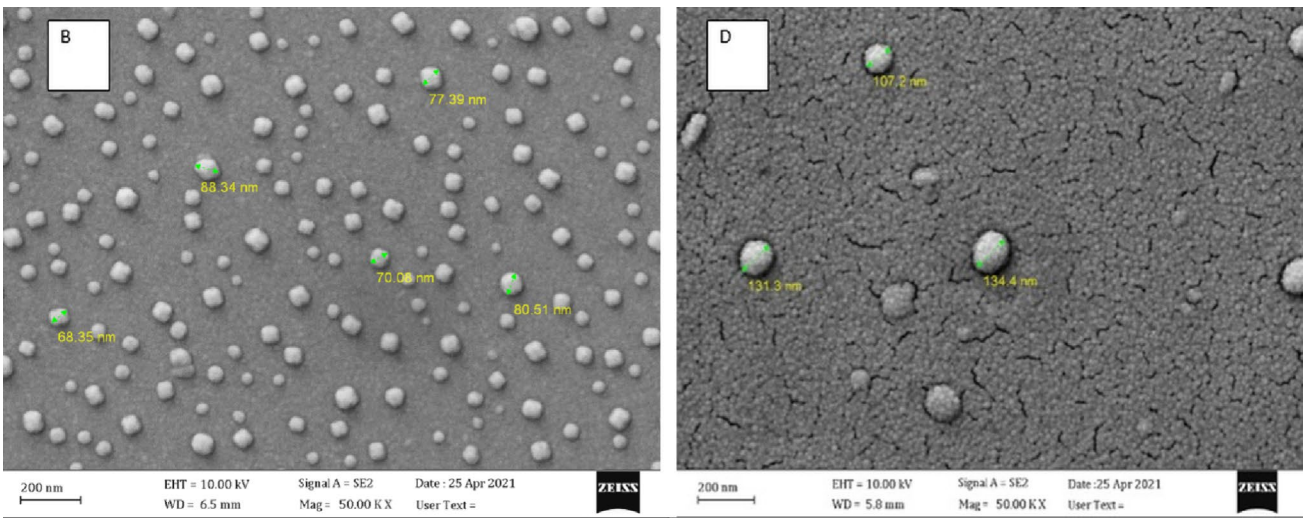

Fig. 5 Field emission scanning microscope (FESEM) image of samples B (ratio 1:4) and D (ratio 1:2) on the left side of the particles made in a double ratio of suspension to iron sulfate salt II. They are smaller in size compared to the particles made in four times the ratio of suspension to salt with a concentration of 0.1 mM

the sample, and in samples with lower salt concentration, the spectrum shifted to shorter wavelengths or blue shift, indicating smaller-sized particles in the sample. Furthermore, in the final concentration of one molar, due to the high concentration of the sample and the low concentration of the suspension in relation to this concentration of our salt, after 10 h, the values were higher than Lambert–Beer's law. We found that to correctly read the absorbance, it was necessary to dilute the sample up to seventy times until the absorbance reached below one and the spectrum was over-scattered.

After this time, as no change was observed in the wave height, the sample was dried in an oven at a temperature of 80 ℃, and the resulting volume was surprisingly small. Therefore, we did not include the sample from this concentration

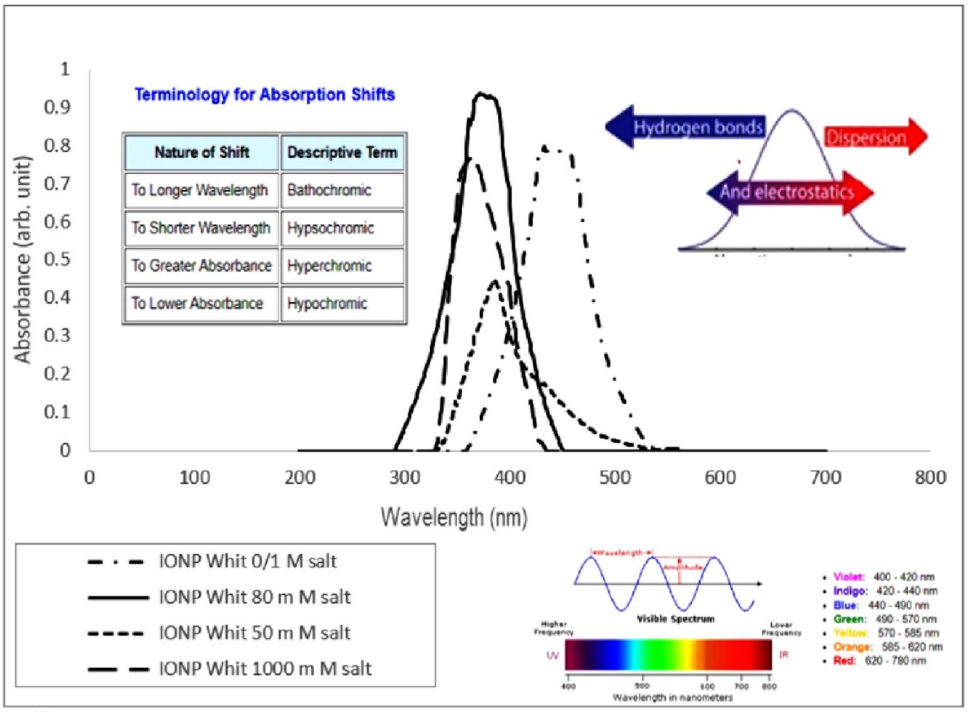

Fig. 6 Visible-ultraviolet light spectroscopy of nanoparticles synthesized from bacterial extracellular suspension and iron sulfate salt in concentrations of 0.1 M, 50, 80, and 1000 mM with a ratio of 2:1

in other characterizations. FESEM imaging and size determination of nanoparticles synthesized at 0.1 M (100 mM) and concentrations of 80 mM and 50 mM were carried out on two scales of 100 nm and 200 nm (Fig. 7). A larger particle size was seen in the sample with a salt concentration of 100 mM (the highest salt concentration selected based on the research of Saravanan et al.) compared to the other samples. Moreover, in concentrations of 80 mM and 50 mM, the visible-ultraviolet light spectroscopy was repeated after one week to check the progress of the reaction; the peak height in the 50 mM sample was not significantly changed. In the other samples, compared to before, to some extent, a hyperchromic shift was seen which, itself, can explain the increase in the molar ratio (ε) according to the Lambert–Beer relation in the sample [47–50]. Because one goal of the current research was to produce the right number of nanoparticles, and because of the proportion of the reducing agent used along with other characteristics of nanoparticles, we did not include the concentration of 50 mM in the following characterizations. The results of Fourier transform infrared spectroscopy characterization of 80 mM and 100 mM samples confirmed the presence of iron nanoparticles in the 545 nm region related to Fe O and the 3470 nm region related to the stretching vibration of the OH group in Fe O (Fig. 8). The intensity of

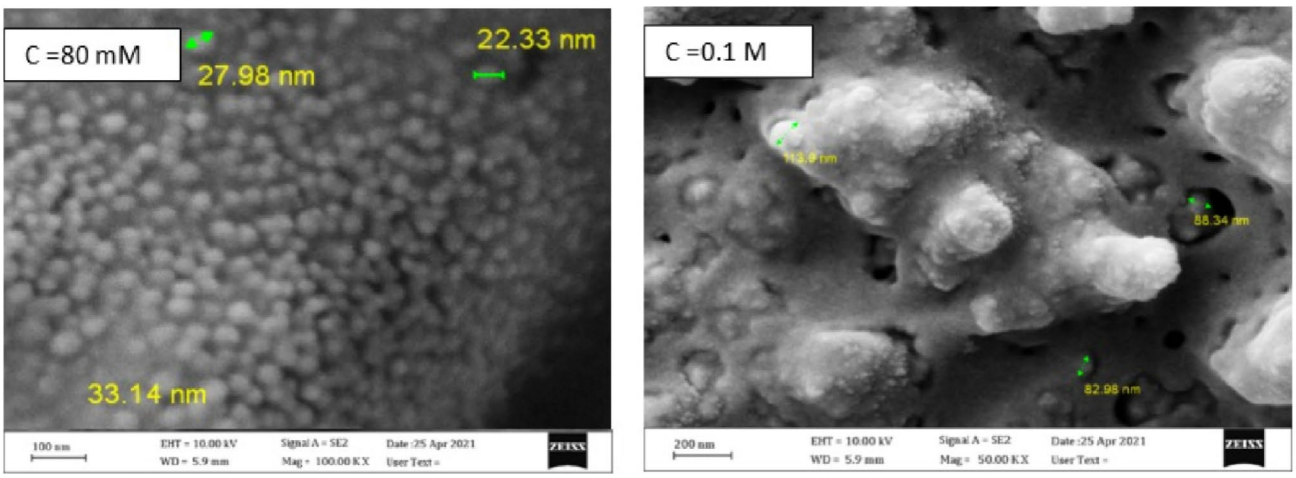

Fig. 7 Field emission scanning microscopy (FESEM)

the Fourier infrared wavelength also confirmed the amount of synthesis of nanoparticles in accordance with the results of ultraviolet–visible light spectroscopy, which revealed that the amount of synthesis at a concentration of 80 mM is more than 100 mM. X-ray energy-dispersive spectroscopy (EDS) (Fig. 9), dynamic light scattering (DLS) (Fig. 10), and zeta potential analysis of nanoparticles were also performed on 80 mM and 100 mM samples (Fig. 11). EDS analysis, as the most common elemental identification method of compounds both qualitatively (i.e., checking the presence or absence of an element in the studied sample) and quantitatively (i.e., checking the presence of each of the elements in the sample), if in the periodic table after boron (bor), was used in the studied sample. Because the elements in our produced nanoparticles had a higher atomic number than carbon and due to the high sensitivity of the detector, this method was used as a secondary technique in determining the quality of the elements in the sample. Electron microscopy, along with FESEM imaging, was used to qualitatively and quantitatively examine the iron and oxygen elements in the produced sample. The results of EDS analysis showed that O and Fe elements are present in all samples, with the sample synthesized with 80 mM salt showing the highest amounts at 23% (Fe) and 8.53% (O). The DLS method is based on the scattering of irradiated light. The frequency of the irradiated light changes over time after hitting the particles in the suspension and has an inverse relationship with the diameter of the particles. All these cases are automatically calculated by the device and output as the multiple scattering index or PDI index (standard deviation squared divided by the average particle diameter). Examining the PDI index of the samples showed that the nanoparticles synthesized with a salt concentration of 80 mM

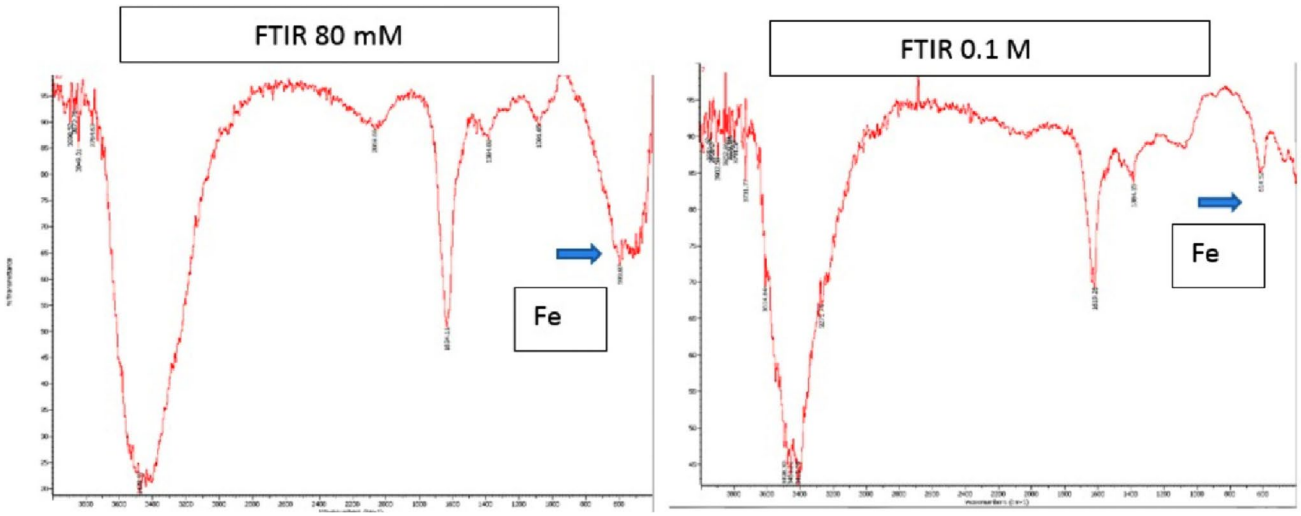

Fig. 8 Fourier transform infrared spectroscopy (FTIR) characterization of synthesized nanoparticles with a final salt concentration of 80 mM and 0.1 M in a volume ratio of 2:1

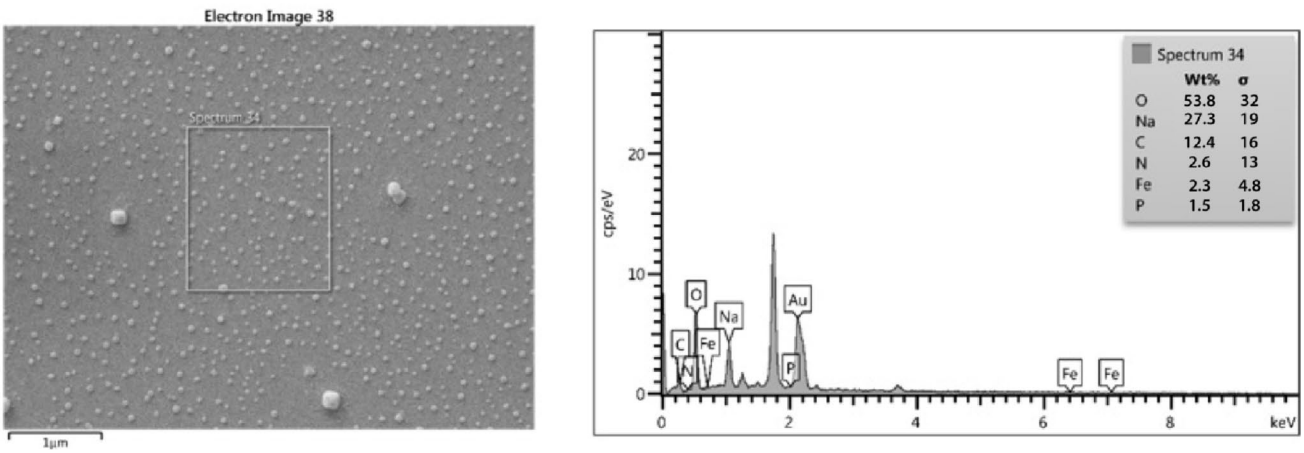

Fig. 9 X-ray energy-dispersive spectroscopy (EDS)

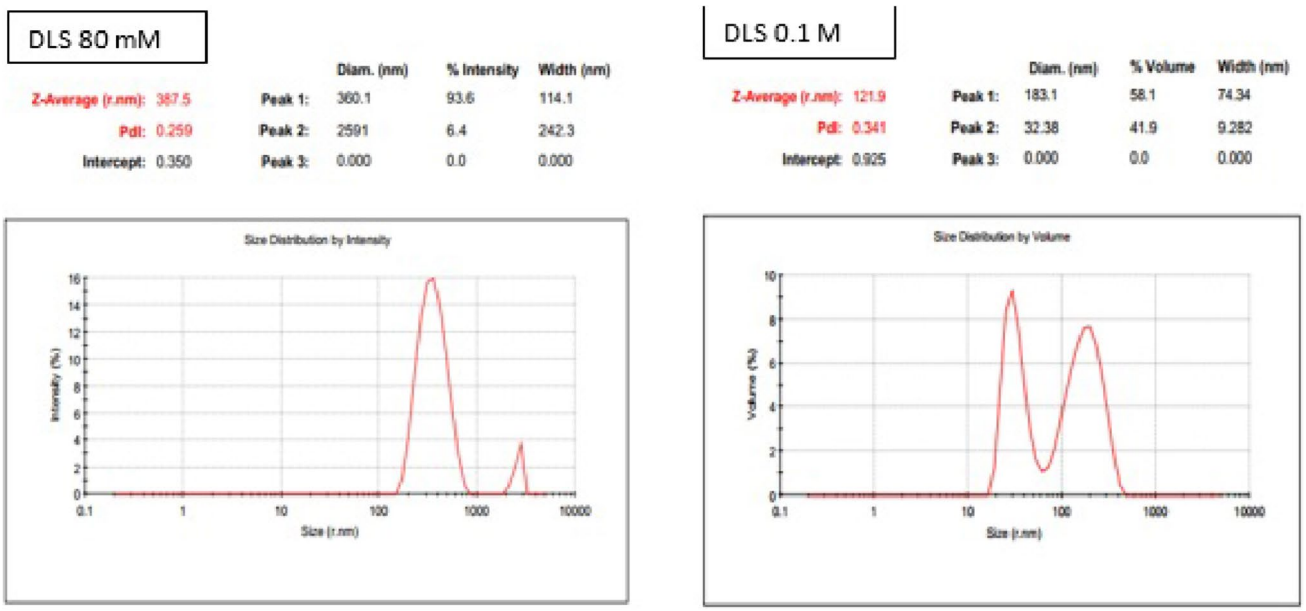

Fig. 10 DLS characterization of synthesized nanoparticles with a final salt concentration of 80 mM and 0.1 M in a volume ratio of 2:1

Fig. 11 Zeta potential of synthesized nanoparticles with a final salt concentration of 80 mM and 0.1 M in a volume ratio of 2:1

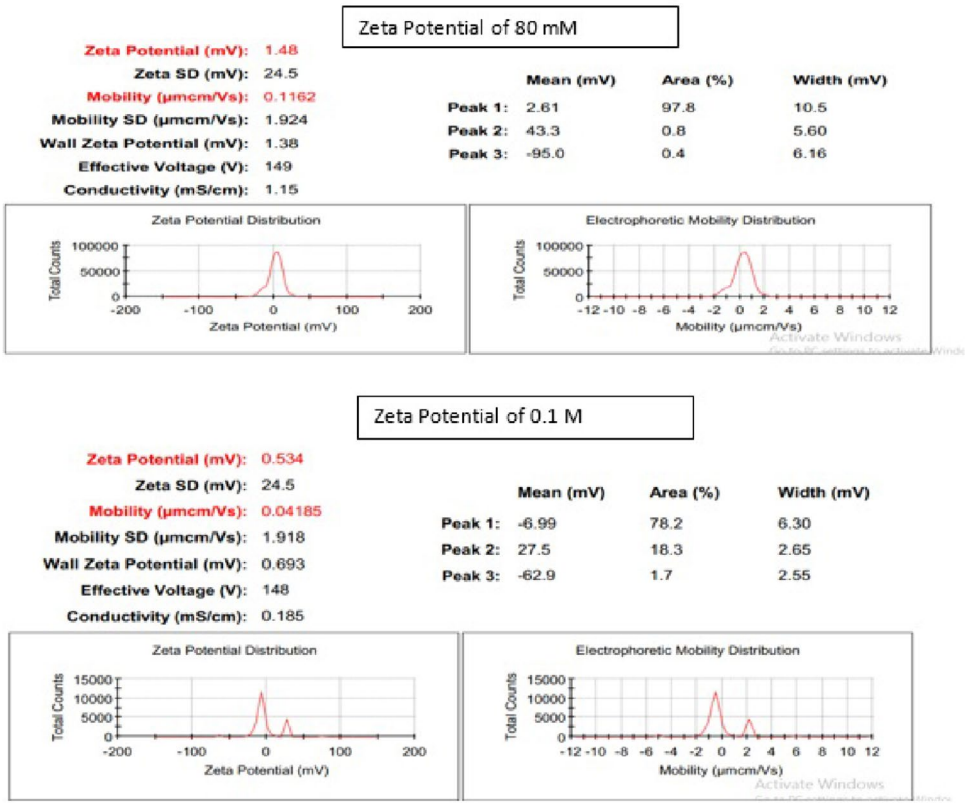

and then 100 mM (0.1 M) had a more favorable PDI in the range close to 0.1 and a more negative/positive zeta potential. Finally, according to the results obtained from the characterization in this research, the samples produced with bacterial suspension cultured in 12-h overnight synthesis at 37 °C with a shaking power of 180 rpm (H2T3S3 sample) and a final concentration of 80 mM of iron II sulfate salt were more favorable than other investigated concentrations. Therefore, other characterizations were carried out on nanoparticles produced with iron II sulfate salt with a concentration of 80 mM.

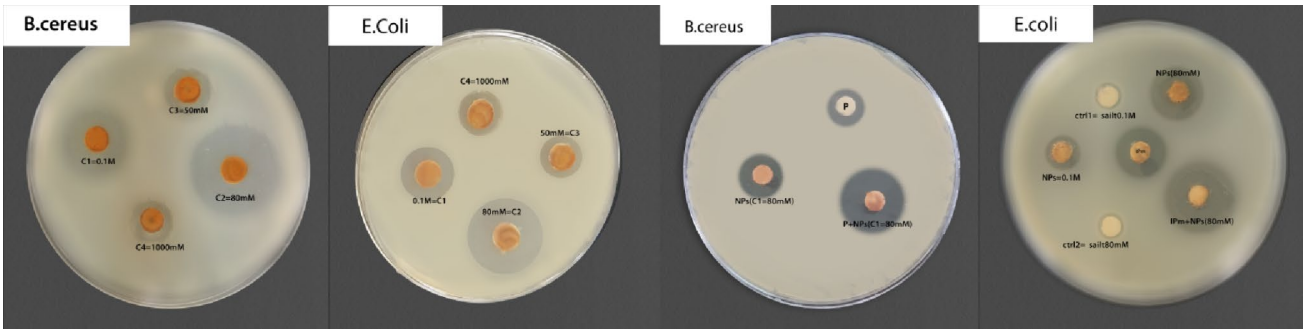

Fig. 12 Antibacterial test by disk diffusion method: diffusion disk impregnated with samples (C1, C2, S1, S2, Fe NPS + P, Fe NPS + IPM) and antibiotic disk on two bacteria, *Bacillus cereus* and *E. coli*, cultivated grass on the plate and halo of lack of growth

Examining the Antibacterial Properties of Synthesized Nanoparticles

Antibacterial Test by Disc Diffusion Method

We evaluated all the synthesized nanoparticles in concentrations of 50 mM, 80 mM, 100 mM, and 1000 mM for antibacterial properties on *E. coli* and *Bacillus cereus* bacteria (two images on the left of Fig. 12). After examining the auras of lack of growth, we found that all nanoparticles had antibacterial properties. After that, we chose two samples of 80 mM and 100 mM, which had a greater and clearer aura of lack of growth, to check the amount of aura of lack of growth in relation to the antibiotic and to check the synergistic effect. As a positive control for *Bacillus cereus*, the antibiotic penicillin and, for *E. coli*, the antibiotic imipenem, were evaluated simultaneously. The non-growth halos for *Bacillus cereus* and *E. coli* bacteria were estimated to be approximately 26 mm and 16 mm, respectively, which are classified as sensitive to nanoparticles based on the CLSI standard. Using Table 3, the results showed that iron oxide nanoparticles have a significant inhibitory effect on *Bacillus cereus* bacteria and *E. coli*. Nonetheless, they are expensive. In addition, the relative comparison of halos revealed a greater impact on *Bacillus cereus* bacteria. To investigate the effect of iron II sulfate salt, we prepared two samples of salt and distilled water in a ratio of 2:1 in two concentrations of 0.1 M (C1) and 80 mM (C2), and discs were impregnated with these two. We also ran the sample on the plates, and in the end, no growth halo was observed compared to these two samples. To investigate the synergistic effect of penicillin and our nanoparticles, along with the discs impregnated with synthesized nanoparticles in salt concentrations of 0.1 M (ctrl 1) and 80 mM (ctrl 2), an antibiotic disc was impregnated with nanoparticles. They were placed on the plate, and the aura of their lack of growth was observed to be 1.5 times larger than the individual state of each of the nanoparticle and antibiotic discs (Fig. 12).

Determining the Minimum Lethal Concentration or MIC

After performing the antibiogram test and taking into account that the lack of growth created by iron oxide nanoparticles synthesized with iron sulfate salt II with a concentration of 80 mM was greater than that created by iron oxide nanoparticles synthesized with sulfate salt, iron II had a concentration of 0.1 mM. The minimum lethality or MIC test was then performed on iron oxide nanoparticles synthesized with iron II sulfate salt with a concentration of 80 mM (S2). The effect of the synthesized nanoparticles on two pathogenic strains was evaluated by the minimum inhibitory concentration (MIC) test, and the results show that in serial dilution using the minimum inhibitory concentration method, iron nanoparticles prevented the growth of the studied bacteria. The minimum

Table 3 Examining the antibacterial property of synthesized nanoparticles in three disc diffusion methods, determination of inhibition concentration, and well diffusion

Bacteria	Antibiotics		Disk release method			Method of determining the minimum lethal concentration	Well release method
	IMP	P	Chemically synthesized nanoparticles	Biomimetic nanoparticle with 0.1 mM salt	Biomimetic nanoparticle with 80 mM salt	Biomimetic nanoparticle with 80 mM salt	Biomimetic nanoparticle with 80 mM salt
B. cereus	21	22	26	25	26	250 M/m	28
E. coli	20	19	23	22	16	500 M/m	20

concentration was confirmed for *Bacillus cereus* bacteria at 250 µg/ml and for *E. coli* at 500 µg/ml (Fig. 13), which confirms the antimicrobial effect of these nanoparticles.

Well Release Method

Inside 4-mm wells, 40 µl (microliters) of the nanoparticle sample produced with the same concentrations that inhibited the growth of *Bacillus cereus* bacteria (250 µg/ml) and *E. coli* (500 µg/ml) in the MIC method and controls were inoculated. The samples were incubated for 24 h at 37 ℃. The diameter of the inhibition halos of the nanoparticles and controls was measured by caliper. The results (Table 3) showed that 250 µg/ml of iron oxide nanoparticles produced from bacterial suspension and iron sulfate II salt could inhibit halo non-growth by as much as 28 ml for *Bacillus cereus* bacteria. Also, 500 µg/ml of the said nanoparticle could create an aura of non-growth of 20 ml for *E. coli* bacteria. This increase in the halo of lack of growth compared to the disking method can be attributed to the removal of the disk as a nanoparticle absorber and the uneven distribution of nanoparticles on both sides of the diffusion disk, which results in reducing the effect on the plate. On the other hand, this increase in diameter of the non-growth halo compared to the non-growth halo of iron oxide nanoparticles synthesized with iron sulfate II salt with a concentration of 0.1 mM can be attributed to the smaller size of the nanoparticles produced with this salt concentration; the increase of the halo of lack of growth, which is a sign of the killing power of bacteria by the tested sample, was related to the change in the size of the nanoparticles. In other words, the nanoparticles synthesized with iron sulfate II salt at a concentration of 80 mM, because they have a smaller size, increased the antibacterial power of these nanoparticles and, thus, the halo. They caused a greater lack of growth compared to the nanoparticles produced with iron II sulfate salt at a concentration of 0.1 mM (Fig. 14).

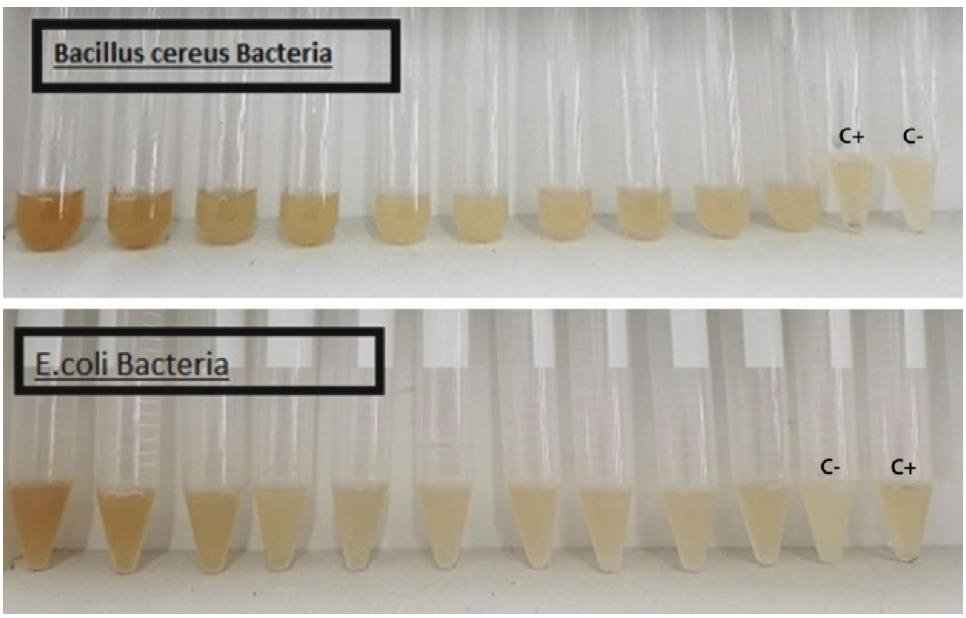

Fig. 13 Determination of the minimum lethality or MIC of iron oxide nanoparticles synthesized with iron sulfate II salt with a concentration of 80 mM on two strains of pathogenic bacteria, *Bacillus cereus* and *E. coli*

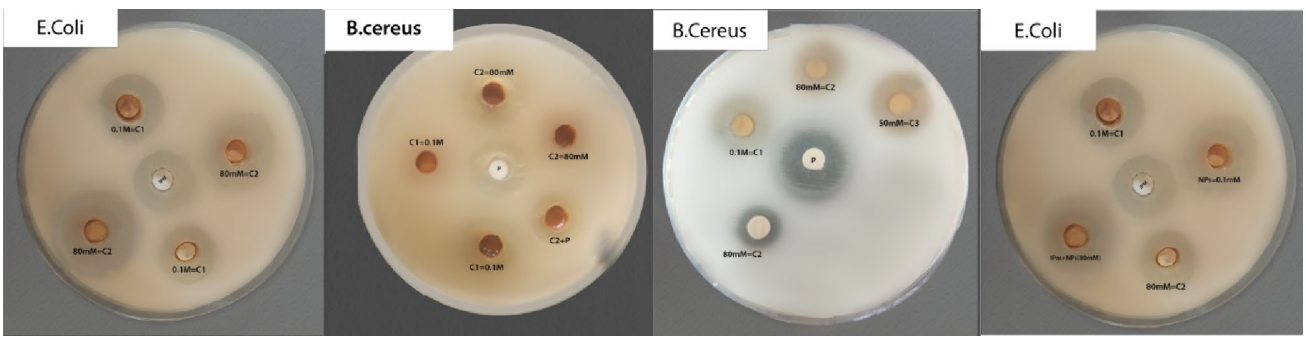

Fig. 14 Antibacterial test by the well release method of iron oxide nanoparticles synthesized with iron sulfate salt II with concentrations of 80 mM and 0.1 M and a sample of salt and distilled water in a ratio of 2:1, in two concentrations of 1 0.0 M (c1) and 80 mM (C2), on two pathogenic strains of *Bacillus cereus* and *E. coli*

Discussion

In the chemical nanoparticle synthesizing methods, increasing the concentration of the reducing agent was reported to decrease the size of nanoparticles. In the biological research, however, salt concentration and extract were reported as factors affecting nanoparticle size. Since nature serves as the inspiration for the synthesis of nano-biota, we stress ethics and principles in scientific research. We think that using living creatures to enhance the quality of human existence should be done in a manner that does not override their lives. For this reason, nano-biota researchers should use mechanisms that create less waste and efficiently use biological resources. We should benefit from them without wasting them and be able to have the maximum use in production with the economical consumption of resources. Therefore, in some parts of the research, the number of nanoparticles produced by bioregenerative agents and the amount of salt consumed as an effective factor in the selection were given particular attention. We tried to first study the concentration of bacterial regenerative agents as an effective biomimetic agent in the synthesis of nanoparticles. In order to determine the concentration of the reducing agent, it was possible to attain the proper concentration of bacteria solely through the examination of physical parameters, including temperature, the duration of the bacteria's night growth, and the quantity of shaker used, without modifying the parameters of the culture medium and effective substances on bacterial growth. Along with collected nanoparticles, the results of measuring the reductive power (DPPH test) of samples showed an increase in the volume of produced nanoparticles. Based on the DPPH test results from the samples, the maximum amount of the effective agent of bioinspiration in the overnight synthesis of 12 h at a temperature of 37 ℃ with a shaking power of 180 rpm (sample H2T3S3) of bacteria was considered the optimal conditions for the growth of bacteria in the continuation of the research for the synthesis of nanoparticles. Until now, this method was not used for the synthesis of iron oxide nanoparticles by other research groups. We could increase the amount of bioinspiration regenerating agent required in the synthesis of iron oxide nanoparticles from *Bacillus megaterium* bacteria to produce smaller nanoparticles without changing the salt concentration (final concentration 0.1 M) and only by optimizing the growth conditions of bacteria and by doing it in the simplest way. Haji Ali et al. could synthesize iron oxide nanoparticles with a size of 20–30 nm from the bioinspiration agents present in *Bacillus megaterium* with a volume ratio of 1:1, and a concentration of 0.1 molar iron sulfate II salt [44], which is the final concentration of salt and the ratio of bacterial suspension to salt. With regard to achieving regenerating agents for synthesis and optimizing bacterial growth conditions, our research diverges from theirs in that we achieved greater success in establishing the properties of the nanoparticles produced. In the second stage of our research, based on the results of optimizing the growth conditions of bacteria (H2T3S3), we studied the concentration of bacterial suspension (bioinspiration regenerating agents), and the final salt concentration in concentrations less than 0.1 M (50 mM and 80 mM), and 1 M concentration (104 times 0.1 M) in the same ratio of 2:1, which was suitable for the final salt concentration of 0.1 M. A volume of nanoparticles produced with a final salt concentration of 1.0 M in a 4:1 ratio and an average size of 130 nm was approximately double that of the nanoparticles produced with this concentration and size, which measured approximately 70 nm in diameter. Although in our previous research we had obtained smaller nanoparticles with a 1:1 ratio of reducing agents and a salt concentration of 0.1, the studies carried out in this research showed that we used a ratio of 2:1 and a 0.1 molar concentration of reducing agent. We were able to use biological and salt optimally because the volume of nanoparticles collected after synthesis was greater at the same time. Therefore, we decided to improve the size of nanoparticles and their other characteristics by changing the salt concentration. Finally, we could produce nanoparticles with an average size of 24 nm and a completely spherical shape at a final concentration of 80 Mm and a ratio of 2:1 for the synthesis of nanoparticles within a week. Considering shape, zeta potential, and PDI index, as well as the amount, the synthesized nanoparticles had better characteristics than iron nanoparticles synthesized in other research, [44–48] and some of them are mentioned in Table 3. In order to assess the caliber of the nano-corn that was generated, standard characterizations were conducted during the nanoparticle synthesis process. This allowed for the reduction in the size of iron oxide nanoparticles to occur in direct proportion to the concentration of the effective bacterial substance while maintaining the volume ratio of the reducing agent iron sulfate I. In the continuation of studies, the antibacterial property of iron oxide nanoparticles was evaluated based on the results obtained in this research. Optimization of the synthesis of iron oxide nanoparticles from the extract of *Bacillus megaterium* bacteria by optimizing the ratio of salt and bacterial suspension and then optimizing the salt concentration was done in an optimized ratio. The iron oxide nanoparticles synthesized in this method are very small (20 to 32 nm) and spherical in shape. It seems that the presence of reducing compounds and enzyme agents in the cytoplasmic extract causes the regeneration of metal ions of iron sulfate II salt and the production of iron oxide nanoparticles. This study, which is a continuation of a previous study by the same group [51], achieved better results than the previous study and those of Ghani et al. by optimizing the ratio of salt and bacterial suspension [52]. To verify

and establish the antibacterial properties of these particles, Ghani et al. (2017) synthesized iron nanoparticles in the range of 40 to 60 nm in diameter after 20 min at room temperature using a suspension of active *Bacillus megaterium* and 0.1 M iron II nitrate salt in a 1:1 ratio. In another study, Fani et al. were able to produce iron oxide nanoparticles from *Lactobacillus fermentum* bacteria from iron sulfate salt III at a concentration of 10–3 M (0.1 M or 100 mM) with an equal volume ratio for three weeks at 37 ℃. Their samples were incubated, and the change in the color of the solution from brick red to black was considered to be favorable for producing iron sulfate nanoparticles [53]. We could achieve smaller nanoparticles with a better DPI index with a lower proportion of salt and a lower concentration than in previous studies (Chart 1).

One of the biggest medical problems is dealing with and eliminating microorganisms that have become resistant to present chemical drugs over time. Increasing the amount of drugs used to deal with resistant bacteria will increase the risk of accumulation of chemicals in the body, cause side effects, and increase their destructive effects on the environment. As a result, investigation into the identification of novel antimicrobial compounds has gained prominence. Certain metals, including silver, zinc, and copper, exhibit antibacterial properties when present in bulk. Conversely, iron oxide lacks antibacterial properties when present in bulk [54]. In 2009, Kawatau et al. reported that cobalt and iron, compared to other metal nanoparticles, such as silver, have better biocompatibility effects and show better anti-inflammatory power, so they can be considered for use as suitable and practical effective agents to deal with and prevent disease factors [55]. Therefore, we decided to study the inhibitory effect of synthesized nanoparticles on pathogenic agents and evaluate the effect of synthesized nanoparticles in different concentrations of suspension and salt, which is effective on their size [40]. The results of our research indicate that synthesized iron oxide nanoparticles showed a suitable antimicrobial effect on gram-positive and gram-negative bacteria. Iron oxide nanoparticles (IONPs) have many practical applications which are synthesized by various methods. IONPs are being studied in terms of their high potential for antimicrobial activity and lack of toxicity to humans [56, 57]. Nevertheless, the variability of IONPs' biological activity is attributable to the synthesis conditions, which also influence their size, structure, and surface modification. This study presents a novel approach to synthesize iron oxide nanoparticles from the bacterium *Bacillus megaterium* in a biomimetic fashion by optimizing physical parameters that have an impact on bacterial growth [58]. By optimizing these parameters during the synthesis of nanoparticles, we could produce disposable nanoparticles with high antibacterial properties without changing the surface [59]. In 2024, Oluwafemi Bamidele Daramola et al. could synthesize iron oxide nanoparticles from gram-positive bacteria extracted from soil. The methodology utilized by the authors indicates that IONP is extracellularly synthesized by six bacterial isolates. The weight percentages of iron bioreduced by *Bacillus subtilis*-A (48%), *Klebsiella aquae*, and pneumoniae are ascertained through energy-dispersive X-ray

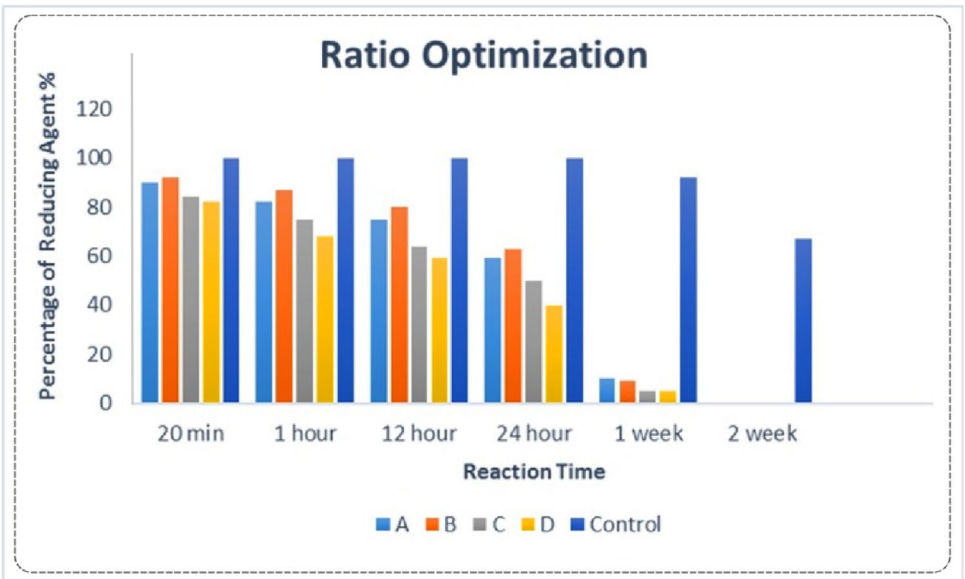

Chart 1 DPPH test results of samples containing suspension and salt with a final concentration of 0.1 M in volume ratios of 1:1 (**A**), 2:1 (**B**), 3:1 (**C**), and 4: 1 (**D**) to determine the optimal duration of synthesis of iron oxide nanoparticles by measuring the salt-reducing power by the biological reducing agents in the bacterial suspension. After centrifuging the samples at certain time intervals, the test of the regeneration power was performed on the supernatant, and the rate of progress of the reaction of each sample along with the control (suspension with a kettle without salt) can be seen

(EDX) spectral analysis. percentage, *Bacillus subtilis*-B (39%), *Bacillus cereus* (38%), *Bacillus badius* (33%), and *Klebsiella africana* (32%). IONPs showed an absorption peak in the range of 250–350 nm, with an average region size of about 72 nm estimated using ImageJ software [60]. We tried to consider the diameter of the non-growth halo as a sign of an antibacterial effect without increasing the concentration of iron oxide nanoparticles. Moreover, to measure and compare the effects of salt concentration and its ratio on the effectiveness of nanoparticles on bacteria, all samples produced with the final concentration of salt, which was produced with a 2:1 ratio of suspension and salt, were tested. Our findings indicate that the nanoparticle samples synthesized with 80 mM salt, followed by 100 mM salt, exhibited superior performance compared to the other samples. This advantage can be attributed to the nanoparticles' size and shape characteristics. In other words, the reduction in the size of iron nanoparticles caused an increase in the surface area, and this increase in the surface area to the volume of nanoparticles can increase the probability of nanoparticles encountering bacterial proteins, or it could be because of the penetration of smaller particles into bacteria, their adverse effect on the vital processes of bacteria, and ultimately their cause of death [33, 54–64].

The results of statistical analysis showed that after comparing two samples of nanoparticles with the positive control group, both samples were significantly different from the positive control group, and with increasing the concentration of salt suspension and decreasing the salt, nanoparticles were produced that caused an increase which had an inhibitory effect on bacteria, despite the fact that in some studies iron nanoparticles have no inhibitory effect on *Escherichia coli* bacteria [65]. Based on the results, the mechanism of the inhibitory effect of iron oxide nanoparticles on *Bacillus cereus* bacteria as a gram-positive bacterium was not significantly different from that on *Escherichia coli* gram-negative bacteria. The degree of cellular toxicity induced by iron oxide nanoparticles is substantially influenced by both the nanoparticle concentration and the specific organism involved. In small concentrations, nanoparticles can act as sources to supply iron ions needed by organisms and improve growth, which seems to be a more useful source of synthesis for the regeneration of salt ions than the source of *Bacillus megaterium* compared to Fermentum [66, 67].

As mentioned earlier, Kandahari et al. and Ghani et al. could produce iron oxide nanoparticles in larger sizes than those produced by us after three weeks of incubation of the suspension and salt. Moreover, the concentration of salt and its ratio with the suspension containing salt ion regenerating agents, which is another factor that affects the size of nanoparticles, was proven by Naguda et al. [40] The current research took this into consideration, which finally caused the production of nanoparticles with a smaller size. This may also account for the nanoparticles' more pronounced inhibitory effect in comparison to the other samples. Gram-positive bacteria have a mucopeptide layer in their cell wall, whereas gram-negative bacteria have lipoprotein and lipopolysaccharide for the majority of their cell wall structure. These bacteria have an outer membrane around their cell wall on one side, and others have enzymes in the periplasmic space (the space between the inner and outer membrane in warm-blooded bacteria, which constitutes approximately 40 to 50% of the volume of the bacteria), which can break down foreign molecules, which is why they are resistant to antibacterial substances; they make them more resistant. Contrary to the present study, however, Khatami et al. reported that iron nanoparticles showed a greater effect on *Escherichia coli* bacteria, [68] and this difference may explain the difference in the shape, size, and concentration of nanoparticles or in terms of the test method [67, 68].

Regarding the possible mechanisms of interactions of nanomaterials with biological macromolecules, the difference between the negative charge of microorganisms and the positive charge of nanoparticles acts as an absorbing electromagnet between the microbe and the nanoparticles. It causes the nanoparticles to connect to the cell surface, and finally, a large number of these contacts lead to oxidation, surface molecules of microbes, and their rapid death [65]. Nanoparticles derived from green chemistry have the potential to serve as a viable substitute for antibiotics in the treatment of microbial infections.

Conclusion

In this research, we were able to make low-cost changes without the intervention of materials and chemical agents, putting the bacteria in conditions of its growth cycle where the salt-reducing agents present in the extracellular suspension of the bacteria have the ability to synthesize more iron oxide nanoparticles. Also, with the help of the biomimetic method, we were able to synthesize nanoparticles without the use of surface modifiers with appropriate reproducibility and with more favorable results on the gram-positive and gram-negative bacteria strains used in the research. By optimizing the synthesis conditions through physical parameters, we were able to reach a more favorable amount of the effective substance for nanoparticle synthesis and also to produce smaller nanoparticles with better properties for therapeutic applications. The results of our characterization show that the nanoparticles produced from the extracellular suspension of *Bacillus megatrium* with a ratio of 2:1 and a salt concentration of 80 mM at room temperature and neutral pH are smaller (27 nm) and more uniform. According to the results of this research, increasing the antibacterial property of produced nanoparticles compared to hospital antibiotics can be beneficial in the treatment of opportunistic hospital infections resistant to current antibiotic treatments. For this purpose, conducting additional research to investigate the in-body characteristics

of these nanoparticles can lead to the development of useful and effective systems in diagnosis and new treatments in the future. So far, various applications of magnetic iron oxide nanoparticles synthesized by different methods have been proven in different fields of medicine by different researchers, with the difference that our synthesis method and antibacterial properties and other features mentioned in this research. Based on the research, it has high innovation. According to the results of the bacterial tests of the synthesized nanoparticles in the mentioned synthesis conditions on *Bacillus cereus* and *Escherichia coli* bacteria, in general, these nanoparticles can be considered suitable candidates for replacing biomimetic nanoparticles instead of common and antibiotic-resistant antibiotics.

Acknowledgements This work is based upon research funded by the Iran National Science Foundation (INSF) under project No. 4020437.

Author Contribution S.H: data curation, formal analysis, investigation, methodology, visualization, writing – original draft. S.D: data curation, formal analysis, investigation, methodology, project administration, supervision, validation, visualization, funding acquisition, writing – review and editing. S.D: data curation, methodology, software, writing – review and editing. Kh.K: visualization, investigation, software, methodology, writing – review and editing.

Data Availability No datasets were generated or analysed during the current study.

Code Availability No custom code was used.

Declarations

Ethics Approval and Consent to Participate This article does not contain any studies with human participants or animals.

Consent for Publication Not applicable.

Competing Interests The authors declare no competing interests.

References

1. Akamatsu R, Suzuki M et al (2019) Novel sequence type in Bacillus cereus strains associated with nosocomial infections and bacteremia, Japan. Emerg Infect Dis 25(5):883
2. Veysseyre F, Fourcade C et al (2015) Bacillus cereus infection: 57 case patients and a literature review. Med Mal Infect 45(11–12):436–440
3. Saif S, Tahir A et al (2016) Green synthesis of iron nanoparticles and their environmental applications and implications. Nanomaterials 6(11):209
4. Atalah J, Espina G et al (2022) Advantages of using extremophilic bacteria for the biosynthesis of metallic nanoparticles and its potential for rare earth element recovery. Front Microbiol 13:855077
5. Yusefi M, Shameli K et al (2021) Green synthesis of Fe3O4 nanoparticles stabilized by a Garcinia mangostana fruit peel extract for hyperthermia and anticancer activities. Int J Nanomedicine 16:2515
6. Tan HL, Lim YC et al (2023) Plant-mediated synthesis of iron nanoparticles for environmental application: mini review. Mater Today Proc 87:64–69
7. Mashjoor S, Yousefzadi M et al (2018) Phycosynthesis of antimicrobial Ulva prolifera-Fe3O4 Magnetic Nanoparticles. Iran J Med Microbiol 12(3):208–217
8. Ge Y, Zhang Y et al (2009) Effect of surface charge and agglomerate degree of magnetic iron oxide nanoparticles on KB cellular uptake in vitro. Colloids Surf B Biointerfaces 73(2):294–301
9. Jahangirian H, Kalantari K et al (2019) A review of small molecules and drug delivery applications using gold and iron nanoparticles. Int J Nanomedicine 14:1633
10. Xia S, Li P et al (2014) In situ precipitation: a novel approach for preparation of iron-oxide magnetoliposomes. Int J Nanomedicine 9:2607
11. Kafali M, Şahinoğlu OB et al (2023) Antibacterial properties and osteoblast interactions of microfluidically synthesized chitosan–SPION composite nanoparticles. J Biomed Mater Res A 111(11):1662–1677
12. Demirezen DA, Yıldız YS et al (2019) Green synthesis and characterization of iron oxide nanoparticles using Ficus carica (common fig) dried fruit extract. J Biosci Bioeng 127(2):241–245
13. Pandey R, Yang FS et al (2023) Comparing the variants of iron oxide nanoparticle-mediated delivery of miRNA34a for efficiency in silencing of PD-L1 genes in cancer cells. Pharmaceutics 15(1):215
14. Devi HS, Boda MA et al (2019) Green synthesis of iron oxide nanoparticles using Platanus orientalis leaf extract for antifungal activity. Green Process Synth 8(1):38–45
15. Kebede A, Gholap AV et al (2011) Impact of laser energy on synthesis of iron oxide nanoparticles in liquid medium. World J Nano Sci Eng 1(4):89–92
16. Ogbezode JE, Ezealigo US et al (2023) A narrative review of the synthesis, characterization, and applications of iron oxide nanoparticles. Discover Nano 18(1):125
17. Spoială A, Ilie CI et al (2023) Smart magnetic drug delivery systems for the treatment of cancer. Nanomaterials 13(5):876
18. Rodriguez-Martinez JA (2010) Improving the in vitro stability of proteins by PEGylation (Doctoral dissertation, University of Puerto Rico, Rio Piedras (Puerto Rico))
19. Dubey SP et al (2010) Lahtinen, Green synthesis and characterizations of silver and gold nanoparticles using leaf extract of Rosa rugosa. Colloids Surf, A Physicochem Eng Asp 364(1–3):34–41
20. Fayaz AM, Girilal M et al (2011) Biosynthesis of anisotropic gold nanoparticles using Maduca longifolia extract and their potential in infrared absorption. Colloids Surf B Biointerfaces 88(1):287–291
21. Ismail EH, Saqer AMA et al (2018) Successful green synthesis of gold nanoparticles using a Corchorus olitorius extract and their antiproliferative effect in cancer cells. Int J Mol Sci 19(9):2612
22. Rajeshkumar S, Malarkodi C et al (2016) Anticancer and enhanced antimicrobial activity of biosynthesized silver nanoparticles against clinical pathogens. J Mol Struct 1116:165–73
23. Setia A, Mehata AK, Malik AK, Viswanadh MK, Muthu MS (2023) Theranostic magnetic nanoparticles: synthesis, properties, toxicity, and emerging trends for biomedical applications. J Drug Delivery Sci Technol 81:104295
24. Tiar OH, Julkapli NM et al (2024) Mechanical performance and fracture surface analysis of fatty acid-coated iron oxide-reinforced nitrile butadiene composites. Polym Bull 81(1):521–533
25. Naveen P, Kaur K et al (2021) Green synthesis: an eco-friendly route for the synthesis of iron oxide nanoparticles. Front Nanotechnol 3:655062
26. Ovejero JG, Armenia I et al (2021) Selective magnetic nanoheating: combining iron oxide nanoparticles for multi-hot-spot induction and sequential regulation. Nano Let 21(17):7213–7220

27. Tran PA, Nguyen HT et al (2018) In vitro cytotoxicity of iron oxide nanoparticles: effects of chitosan and polyvinyl alcohol as stabilizing agents. Mater Res Express 5(3):035051
28. Ashrafizadeh M, Zarrabi A et al (2023) (Nano) platforms in breast cancer therapy: drug/gene delivery, advanced nanocarriers and immunotherapy. Med Res Rev 43(6):2115–2176
29. Virtanen PS, Ortiz KJ, Patel A, Blocher WA, Richardson AM (2024) Blood–brain barrier disruption for the treatment of primary brain tumors: advances in the past half-decade. Curr Oncol Rep 1–14
30. Khan MJ, Karim Z (2021) Starch magnetic nanocomposites for gene delivery. In: polysaccharide-based nanocomposites for gene delivery and tissue engineering. Woodhead Publishing 295–309
31. Bhandari V, Jose S et al (2022) Antimicrobial finishing of metals, metal oxides, and metal composites on textiles: a systematic review. Ind Eng Chem Res 61(1):86–101
32. Zambri NDS, Taib NI et al (2019) Utilization of neem leaf extract on biosynthesis of iron oxide nanoparticles. Molecules 24(20):3803
33. Fani M, Ghandehari F et al (2018) Biosynthesis of iron oxide nanoparticles by cytoplasmic extract of bacteria lactobacillus fermentum. J Med Chem Sci 1(2):28–30
34. Huang KC, Ehrman SH et al (2007) Synthesis of iron nanoparticles via chemical reduction with palladium ion seeds. Langmuir 23(3):1419–1426
35. Huber DL (2005) Synthesis, properties, and applications of iron nanoparticles. Small 1(5):482–501
36. Logan NA, Rodríguez-Díaz M (2006) Bacillus spp. and related genera. Principles and Practice of Clinical Bacteriology 139–158
37. Mondal A, Mukherjee A, Pal R (2023) Phycosynthesis of nanoiron particles and their applications-a review. Biocatal Agric Biotechnol 102986
38. Borriss R (2020) Bacillus. In Beneficial microbes in agro-ecology. Academic Press 107–132
39. Magiorakos AP, Srinivasan A et al (2012) Multidrug-resistant, extensively drug-resistant and pandrug-resistant bacteria: an international expert proposal for interim standard definitions for acquired resistance. Clin Microbiol Infect 18(3):268–281
40. Nadagouda MN, Castle AB, Murdock RC, Hussain SM, Varma RS (2010) In vitro biocompatibility of nanoscale zerovalent iron particles (NZVI) synthesized using tea polyphenols. Green Chem 12(1):114–122
41. Saravanan M, Gopinath V et al (2018) Green synthesis of anisotropic zinc oxide nanoparticles with antibacterial and cytofriendly properties. Microb Pathog 115:57–63
42. Wang N, Hsu C et al (2013) Influence of metal oxide nanoparticles concentration on their zeta potential. J Colloid Interface Sci 407:22–28
43. Cho WS, Duffin R et al (2012) Zeta potential and solubility to toxic ions as mechanisms of lung inflammation caused by metal/metal oxide nanoparticles. Toxicol Sci 126(2):469–477
44. Bhattacharjee S (2016) DLS and zeta potential–what they are and what they are not? J Control Release 235:337–351
45. Cursaru LM, Piticescu RM et al (2020) The influence of synthesis parameters on structural and magnetic properties of iron oxide nanomaterials. Nanomaterials 10(1):85
46. Gutiérrez L, De la Cueva L et al (2019) Aggregation effects on the magnetic properties of iron oxide colloids. Nanotech 30(11):112001
47. Gutiérrez L, De la Cueva L et al (2011) Near infra red spectroscopy—an overview. Int J ChemTech Res 3(2):825–836
48. Budzak S, Laurent AD et al (2016) Solvatochromic shifts in UV–Vis absorption spectra: the challenging case of 4-nitropyridine N-oxide. J Chem Theory Comput 12(4):1919–1929
49. Akash MSH, Rehman K, Akash MSH, Rehman K (2020) Ultraviolet-visible (UV-VIS) spectroscopy. Essentials of Pharmaceutical Analysis 29–56
50. Rance GA, Marsh DH et al (2010) UV–vis absorption spectroscopy of carbon nanotubes: relationship between the π-electron plasmon and nanotube diameter. Chem Phys Lett 493(1–3):19–23
51. Hajiali S, Daneshjou S et al (2022) Biomimetic synthesis of iron oxide nanoparticles from Bacillus megaterium to be used in hyperthermia therapy. AMB Express 12(1):145
52. Ghani S, Rafiee B et al (2017) Biosynthesis of iron nano-particles by Bacillus megaterium and its anti-bacterial properties. J Babol Univ Med Sci 19(7):13–19
53. Fani M, Ghandehari F et al (2019) Study on the antimicrobial effects of iron oxide nanoparticles synthesized by cytoplasmic extract of lactobacillus fermentum. New Cell Mol Biotech J 9(36):89–96
54. Seil JT (2012) Webster, Antimicrobial applications of nanotechnology: methods and literature. Int J Nanomedicine 7:2767
55. Khatami M, Aflatoonian MR et al (2017) Evaluation of antibacterial activity of iron oxide nanoparticles against Escherichia coli. Int J Basic Sci Med 2(4):166–169
56. Harikrishnan AM, Chowdhury ZZ, Rana M, Ali AE, Mitra A, Rafique RF, Johan RB (2024) Green synthesis of iron oxide nanoparticles and its application in water treatment. In wastewater treatment using green synthesis. CRC Press 28–46
57. ScafaUdriște A, Burdușel AC et al (2024) Metal-based nanoparticles for cardiovascular diseases. Int J Mol Sci 25(2):1001
58. Flieger J, Pasieczna-Patkowska S et al (2024) Characteristics and antimicrobial activities of iron oxide nanoparticles obtained via mixed-mode chemical/biogenic synthesis using spent hop (Humulus lupulus L.) extracts. Antibiotics 13(2):111
59. Daramola OB, George RC et al (2024) Insights on the synthesis of iron-oxide nanoparticles and the detection of iron-reducing genes from soil microbes. Colloids Surf C: Environ Aspect 2:100025
60. Khatoon N, Alam H et al (2019) Ampicillin silver nanoformulations against multidrug resistant bacteria. Sci Rep 9(1):6848
61. Wang L, Hu C, Shao L (2017) The antimicrobial activity of nanoparticles: present situation and prospects for the future. Int J Nanomed 1227–1249
62. Gabrielyan L, Trchounian A (2019) Antibacterial activities of transient metals nanoparticles and membranous mechanisms of action. World J Microbiol Biotechnol 35:162
63. Khatoon N, Alam H et al (2019) Silver-coated magnetic nanocomposites induce growth inhibition and protein changes in foodborne bacteria. Sci Rep 9(1):17499
64. Torabian P, Ghandehari F et al (2019) Evaluating antibacterial effect of green synthesis oxide iron nanoparticles using cytoplasmic extract of Lactobacillus casei. J Babol Univ Med Sci 21(1):237–241
65. Zhang L, Jiang Y et al (2007) Investigation into the antibacterial behaviour of suspensions of ZnO nanoparticles (ZnO nanofluids). J Nanopartic Res 9(3):479–89
66. Vazquez-Muñoz R, Avalos-Borja M et al (2014) Ultrastructural analysis of Candida albicans when exposed to silver nanoparticles. PLoS One 9(10):e108876
67. Mishra D, Arora R et al (2014) Synthesis and characterization of iron oxide nanoparticles by solvothermal method. Prot Met Phys Chem 50(5):628–631
68. Emamifar A, Kadivar M et al (2011) Effect of nanocomposite packaging containing Ag and ZnO on inactivation of Lactobacillus plantarum in orange juice. Food Control 22(3–4):408–413